Optical Characterization of Electron Beam Evaporated Indium Antimonide Thin Films

Rahul*, A. K. Verma, R. S. N. Tripathi and S. R. Vishwakarma Department of Physics & Electronics, Dr. R M L Avadh University, Faizabad, India

The non-stoichiometric ($In_{0.66}Sb_{0.34}$) thin films of 300 nm thickness were deposited at different temperatures onto well cleaned glass substrates by electron beam evaporation technique at different substrate temperatures. Optimized composition ($In_{0.66}Sb_{0.34}$) is used for fabrication of thin films. These films have polycrystalline nature with zinc blende structure and oriented along (111) and (220) planes. The decrease in electrical resistivity with increasing temperature shows semiconducting behavior. Optical absorption spectrums of deposited thin films have been recorded using FTIR spectrophotometer. Direct band gap has been determined using these spectra.

1. Introduction

The preparation and characterization of nonstoichiometric indium antimonide (In_{0.66}Sb_{0.34}) thin films plays a major role in scientific research and its application. Among the III-V binary compound semiconductors, indium antimonide shows n-type or p-type semi-conductivity, polycrystallinity and melting point of 798 K. It is a narrow-band-gap semiconductor with an energy band gap of 0.17 eV at 300 K and 0.23 eV at 80 K [1-3]. In n-type indium antimonide (anion vacancy), the electrons have high mobility (80,000 cm²/Vs) due to their smaller effective mass. Similarly, in p-type InSb (cation vacancy), the holes have the mobility of 1250 cm²/Vs. Therefore, InSb is a material suitable for magnetic-field sensing devices such as Hall sensor and magnetoresistors [4], speed-sensitive sensors [5] and magnetic sensors [6]. The infrared detectors fabricated from n-type InSb thin films are sensitive between 3-5 µm wavelengths [7]. These n-type InSb thin films can also be used as biosensor to detect bacteria. Many reports are available on the growth of InSb thin films using different deposition techniques such as molecular beam epitaxy (MBE) [8], metal organic chemical vapor deposition (MOCVD) [9], vacuum evaporation [10], liquid phase epitaxy [11], and sputtering [12]. The non-stoichiometry in the structure or vacancies in thin films of indium antimonide is created during the deposition process. The anion vacancies, i.e., indium enriched, exhibit n-type semi-conductivity and the cation vacancies exhibit p-type semi-conductivity due to excess of antimony. The aim of present study is to

fabricate non-stoichiometric n-type indium substrate antimonide thin films at different temperatures and the characterized properties. Indium enriched non-stoichiometric InSb, a powder with the composition of In_{0.66}Sb_{0.34} is used for the fabrication of thin films. This composition of indium and antimony in material has been optimized on the basis of electrical, optical and structural properties [13, 14]. This is a novel method to create controlled amount of nonstoichiometry in thin films. We have fabricated ntype InSb thin films by electron beam evaporation technique using aforesaid materials having a controlled non-stoichiometric composition. The electron beam evaporation technique is more suitable than physical evaporation techniques because, during the deposition the materials come into vapor state without changing into liquid state.

2. Experimental Details

2.1. Substrate cleaning

The substrate cleaning plays an important role in the deposition of thin films, so commercially available glass substrates with the size of (75 mm x 25 mm x 1mm), were washed in detergent then in chromic acid and finally washed with double distilled water in ultrasonic cleaner and dried at 423 K in an oven.

2.2. Preparation of starting materials

Indium and antimony metal powders with 99.999% purity have been purchased from Alfa-Aesar Ltd. USA. The non-stoichiometric starting materials had the composition $In_{0.66}Sb_{0.34}$. Desired molar ratios of $In_{0.66}$ (indium) and $Sb_{0.34}$ (antimony) metal powders

^{*}rhl.jaunpur@gmail.com

were mixed by grinding with a mortar rod and then the mixed powder was heated at 323 K in a vacuum unit (Hind Hivac Company. Ltd, India) using molybdenum boat under a vacuum of $\sim 2 \times 10^{-5}$ torr for ten hours and cooled down to room temperature under the same vacuum conditions. The cooled sample was again grinded with the mortar rod and heated under the same vacuum conditions. This process was repeated five times at different temperatures greater than 323K for formation of crystalline InSb.

2.3. Preparation of thin films

The non-stoichiometric ($In_{0.66}Sb_{0.34}$) thin films of 300 nm thickness were deposited at different temperatures onto well cleaned glass substrates by electron beam evaporation technique under vacuum of 10^{-5} torr. The prepared aforesaid non-stoichiometric starting material was taken in a graphite crucible and evaporated in vacuum ($\sim 10^{-5}$ torr) in the vacuum system equipped with liquid nitrogen trap. The source materials were kept at the distance of 125 mm from the substrate holder. The deposition rate (3.0-18 nm/s) was adjusted by changing the electrical current of electron beam gun. The deposition rate was measured by digital film thickness monitor using a quartz crystal sensor set at 6 MHz (DTM-10).

2.4. Structural and electrical characterization

The X-ray Diffractogram of non-stoichiometric thin films was obtained by using the Philips Analytical X-ray Diffractometer (PW-3710) operated at 40 kV/20 mA using CuK $_{\alpha l}$ radiation with the wavelength of 1.5404 Å in the angle region from 20° to 70° at Jamia Milia Isalamia University, New-Delhi. The measurement of electrical resistivity of the non-stoichiometric indium antimonide thin film has been done using a standard four-probe method and the Hall Effect study is used to recognize the n- or p-type semiconductor.

2.5. Optical characterization

Optical absorption and transmittance of InSb thin films was recorded using Fourier transform infrared spectrophotometer (FTIR) model No. Jasco/4100 with the wave length range of 2000-4000 nm, from the Department of Physics, The M S University, Vadodara (Gujrat). From the transmission data, the absorption coefficient (α) is calculated for all deposited thin films in the region of strong absorption using the relation [15]

$$\alpha = \frac{1}{d} \ln \left(\frac{1}{T} \right)$$

Where, α is absorption coefficient at particular wavelength, T is transmittance at same wavelength and d is film thickness.

The optical energy band gap of thin films is calculated by using Tauc relation [16]

$$\alpha h \nu = A(h \nu - Eg)^n$$

Where, $h \nu$ is Photon energy, Eg is Optical band gap, A is constant, $n = \frac{1}{2}$ for direct band gap material.

3. Result and Discussions

3.1. Structural and electrical analysis of InSb thin films

Figs. 1(a,b,c) show the X-ray diffraction pattern of non-stoichiometric InSb thin film with different temperature. The presence of sharp peak in XRD pattern confirmed the polycrystalline nature having zincblende structure and oriented along (111) and (220) planes. This is confirmed by comparing the observed values of the XRD patterns of films with the standard 'd' values of JCPDS X-ray powder file data (Card No.PDF#06-0208) and given in Table 1. As the deposited temperature of thin films increases, the intensity of (111) plane increases with (220) plane. This indicates that full-width half maxima (β) of the XRD peaks decreases with temperature and increases the grain size of the films. Fig. 2 shows the variation of resistivity with substrate temperature. It is clear from Fig. 2 that the resistivity of deposited films decreases with substrate temperature. This may be due to bigger crystallite size in the film at higher temperature as compared to the film deposited at lower substrate temperature. Similar result obtained by other investigators [17]. Hall Effect measurement shows that the deposited films are n-type semi conductivity.

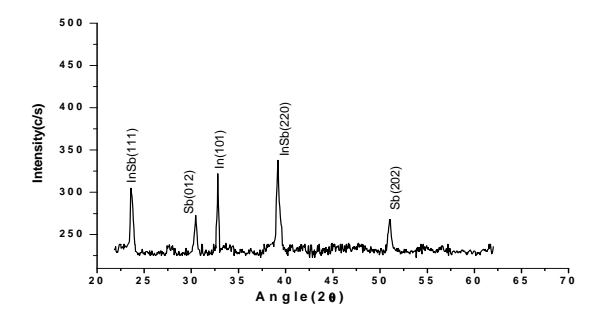


Fig.1(a): X-ray diffraction pattern of as deposited films at 300K.

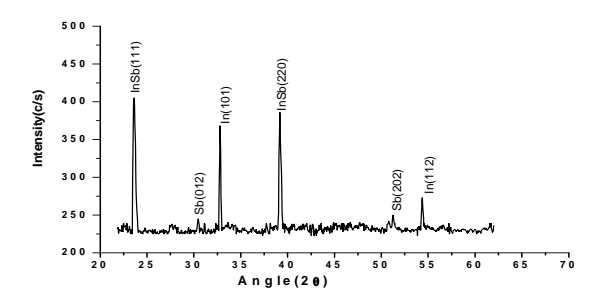


Fig.1(b): X-ray diffraction pattern of as deposited films at 323K

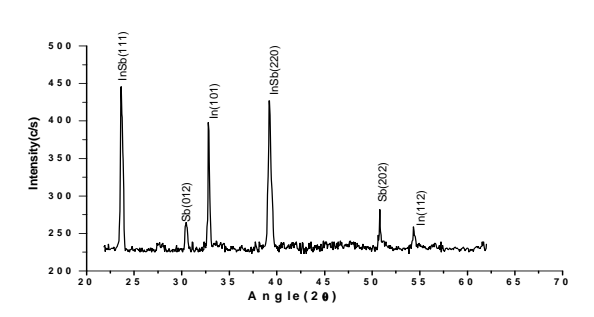


Fig.1(c): X-ray diffraction pattern of as deposited films at 373K.

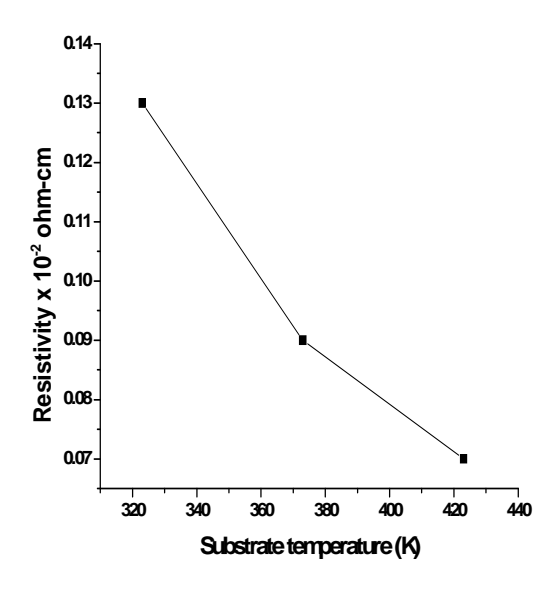


Fig.2: Variation of resistivity with substrate temperature of as deposited film.

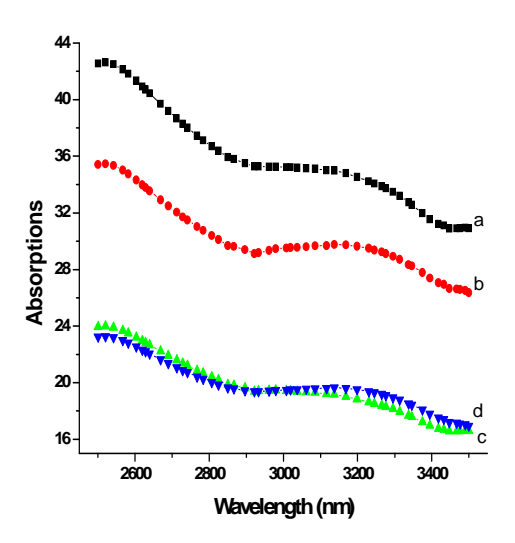


Fig.3: Wavelength versus absorption spectrum of as deposited thin films for temperature (a) 300K (b) 323K (c) 373K (d) 423K.

Table 1: Experimental and standard d-value of InSb.

S. No	Diffraction angle	(h k l) plane	Observed d value	Standard d
	(2θ)		(Å)	value (Å)
1.	23.84	(111)	3.751	3.740
2.	39.17	(220)	2.287	2.290
3.	56.66	(400)	1.619	1.620
4.	46.38	(311)	1.952	1.953
5.	76.33	(511)	1.247	1.247

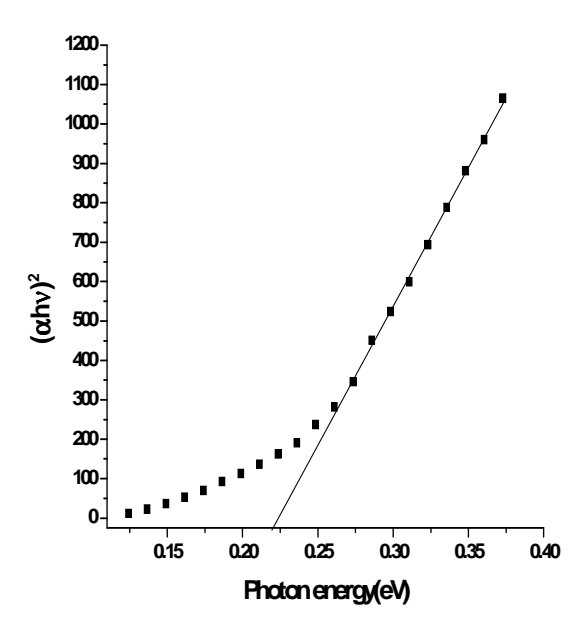


Fig.4: Photon energy versus ($\alpha h v$)² of as deposited thin films for temperature 300K.

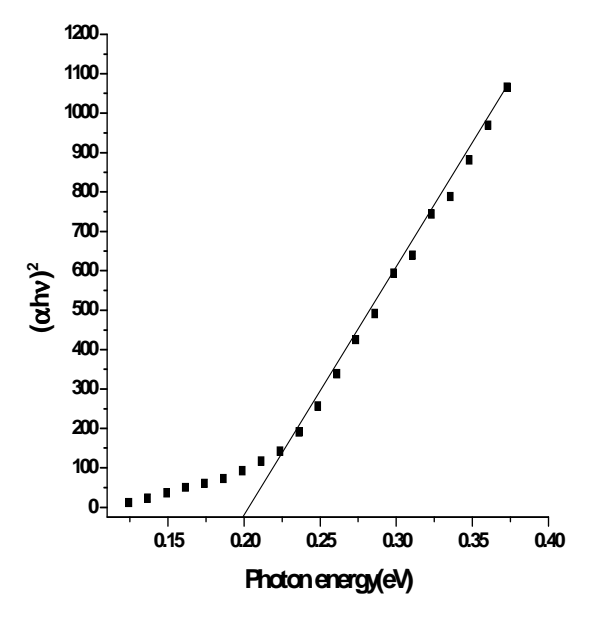


Fig.5: Photon energy versus ($\alpha h v$)² of as deposited thin films for temperature 323K.

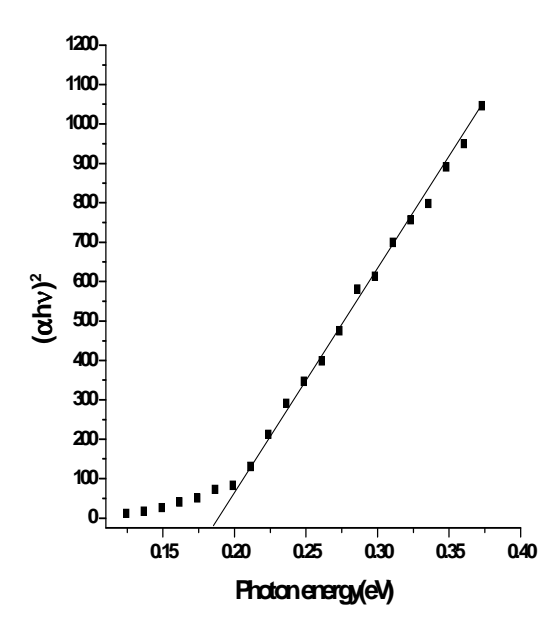


Fig.6: Photon energy versus ($\alpha h v$)² of as deposited thin films for temperature 373K.

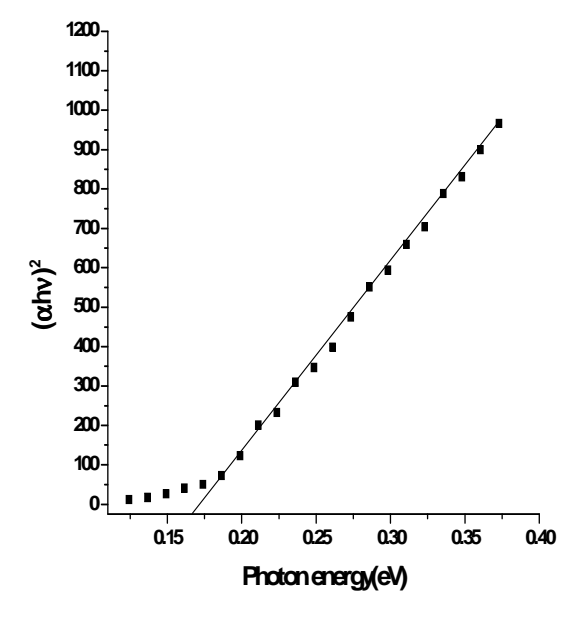


Fig.7: Photon energy versus ($\alpha h v$)² of as deposited thin films for temperature 423K.

3.2. Optical analysis of InSb thin films

Fig. 3 shows wavelength versus absorption spectra of deposited non-stoichiometric thin films. It is clear from Fig. 3 that the optical absorption decreases and transmittance increases with the increase of wavelength. The result of InSb thin films deposited at 300K, 323K, 373K and 423K, respectively, revealed that the transmittance increases with an increase in the temperature of thin film deposition (Fig. 3). The as deposited (room temperature, 300K) film has nano-crystalline structure and has a large number of grain boundaries. The grain boundary reflections results in more scattering of infrared radiation in the films [17, 18]. The scattered light has more chances to be absorbed by the films. Therefore, a reduction in transmittance is observed for the as deposited films. As the temperature of deposition is increased (323K, 373K and 423K), only thermodynamically stable phase are present, in addition to this the grains also coarsen resulting in the reduction of grain boundaries. This decrease in grain boundary areas will reduce the scattering of the infrared radiation in the films and consequently will result in an increase in the transmittance.

Figs. 4-7 show a variation of $(\alpha h v)^2$ with photon energy for non-stoichiometric InSb thin films of 300nm thickness at different temperature. It is clear from Figs. 4-7 that the extrapolation of straight-line portion to $(\alpha h v)^2 = 0$ axis gives the value of direct band gap. It is observed from Figs. 4-7 that the direct band gaps have values 0.22 eV, 0.20 eV, 0.18 eV, and 0.16 eV, respectively. The observed optical direct band gap can be explained on the basis of the reduction in the number of unsaturated defects and the decrease in density of localized state in the band structure of the films [16]. These direct band gap obtained in present investigation are in agreement with the observation by other investigators [1, 3, 17].

4. Conclusions

Non-stoichiometric indium antimonide thin films of 300nm thickness were deposited at different temperature on well cleaned glass substrate by electron beam evaporation technique. The x-ray diffraction pattern shows that these films have polycrystalline nature with zinc blende structure and oriented along (111) and (220) planes, respectively. The decrease in electrical resistivity with increasing temperature shows semiconducting behavior. From the optical absorption spectra, it was found that absorption decreases and transmittance increases at deposition temperature.

Direct band gap have values of the films equal to 0.16-0.22eV.

Acknowledgments

The financial support has been provided by U.P, Council of Science & Technology, Lucknow, India. Authors are thankful to Prof. K. Singh, Department of Physics & Electronics, Dr. R.M.L Avadh University, Faizabad, for providing necessary facilities. Authors are also thankful to the Prof. N. L. Singh, M.S. University, Vadodara for providing the facility of FTIR measurement and Dr. Shree Ram Vishwakarma for useful discussions.

References

- [1] R. K. Mangal and Y. K. Vijay, Bull. Mater. Sci. **30**, 117 (2007).
- [2] R. K. Mangal, B. Triapthi, M. Singh, Y. K. Vijay and A. Rais, Indian J. Pure & Applied Phys. 45, 987(2007).
- [3] R. K. Mangal, Y. K. Vijay, D. K. Avatshi and B. R. Shekhar, Indian J. Engin. & Mater. Sci. 14, 253 (2007).
- [4] J. Heremans, D. L. Partin and C. M. Thrush, Semi Sci. Technol. **8**, 424 (1993).
- [5] M. K. Carpenter and M. W. Verbrugge, J. Mater. Res. 9, 2584 (1994).
- [6] A. Okamoto, T. Yoshida, S. Muramatsu and I. Shibasaki, J. Cryst. Growth 201, 765 (1999).
- [7] N. K. Udayshankar and H. L. Bhat, Bull. Mater. Sci. 24, 445 (2001).
- [8] T. Zhang, S. K. Clowes, M. Debnath, A. Bennett, C. Roberts, J. J. Harris and R. A. Stradling, Appl. Phys. Lett. 84, 22 (2004).
- [9] D. K. Gaskill, G. T. Stauf and N. Bottka, Appl. Phys. Lett. 58, 1905 (1991).
- [10] M. A. Taher, Daffodil International University Journal of Science and Technology **2**, 39 (2007).
- [11] D. E. Holunes and G. S. Kamnath, J. Electron Mater. **9**, 95 (1980).
- [12] T. Miyazaaki, M. Kunugi, Y. Kitamure and S. Adachi, Thin Solid Films **287**, 51 (1996).
- [13] S. R Vishwakarma, A. K Verma, R. S. N. Tripathi, S. Das and Rahul, Indian J. Pure & Applied Phys. 50, 346 (2012).
- [14] S. R. Vishwakarma, A. K. Verma, R. S. N. Tripathi and Rahul, Proc. Natl. Acad. Sci., India, Sect. A Phys. Sci. 82, 245 (2012), DOI 10.1007/s40010-012-0031-y
- [15] C. Mehta, J. Abass, G. Saini and S. Tripathi, Chalcogenide Letter 11, 133 (2007).
- [16] M. Singh and Y. K. Vijay, Indian J. Pure & Applied Phys. 42, 610 (2004).

- [17] S. Singh, K. Lal, A. K. Srivastava, K. N. Sood and Ram Kishore, Indian J. Engin. & Mater. Sci. **14**, 55 (2007).
- [18] S. Singh, A. K. Srivastava, K. Lal, Y. Tomokiyo, S. K. Sharma and R. Kishore, Indian J. Engin. & Mater. Sci. 13, 339 (2006).

Received: 12 February, 2012 Accepted: 21 September, 2012